



Heriot-Watt University
Research Gateway

Effects of Orifice Diameter and Retention Time of Local Tanks on the Reliability and Carbon Footprint of Water Distribution Networks

Citation for published version:

Rizvi, S, Rustum, R, Giustolisi, O, Wright, G, Arthur, S & Berardi, L 2021, 'Effects of Orifice Diameter and Retention Time of Local Tanks on the Reliability and Carbon Footprint of Water Distribution Networks', *Journal of Water Resources Planning and Management*, vol. 147, no. 11, 05021023. [https://doi.org/10.1061/\(ASCE\)WR.1943-5452.0001468](https://doi.org/10.1061/(ASCE)WR.1943-5452.0001468)

Digital Object Identifier (DOI):

[10.1061/\(ASCE\)WR.1943-5452.0001468](https://doi.org/10.1061/(ASCE)WR.1943-5452.0001468)

Link:

[Link to publication record in Heriot-Watt Research Portal](#)

Document Version:

Peer reviewed version

Published In:

Journal of Water Resources Planning and Management

Publisher Rights Statement:

This material may be downloaded for personal use only. Any other use requires prior permission of the American Society of Civil Engineers. This material may be found at: [https://doi.org/10.1061/\(ASCE\)WR.1943-5452.0001468](https://doi.org/10.1061/(ASCE)WR.1943-5452.0001468)

General rights

Copyright for the publications made accessible via Heriot-Watt Research Portal is retained by the author(s) and / or other copyright owners and it is a condition of accessing these publications that users recognise and abide by the legal requirements associated with these rights.

Take down policy

Heriot-Watt University has made every reasonable effort to ensure that the content in Heriot-Watt Research Portal complies with UK legislation. If you believe that the public display of this file breaches copyright please contact open.access@hw.ac.uk providing details, and we will remove access to the work immediately and investigate your claim.

26 **Abstract**

27 The role of private tanks is to provide excessive storage to the consumer to satisfy the water demand.
28 However, they are disregarded during the design stage, in favor of simplified network analysis. This affects the
29 accuracy of the simulation as vital components, such as tank's inlet and volume sizes, are completely ignored. Hence,
30 the purpose of this study is to demonstrate the effectiveness of advanced modelling of WDN, encompassing the
31 presence of local private tanks, to determine the optimum values of different parameters of private tank by conducting
32 time and volume-based reliability analysis. Two network models are used to perform the analysis: a small sample
33 network and a real network that resembles the area of Dubai Silicon Oasis, Dubai, UAE. The results obtained from
34 the simulation of networks indicated that the lowest orifice and volume size(s) to achieve the required reliability of
35 unity is the optimum values. Furthermore, it implied that any change in their optimum values would either result in
36 tank failure or increase in the head loss and carbon footprint of the network.

37 **Keyword(s):** *Water distribution network; Reliability analysis; Private tanks; Orifice diameter; Carbon Footprint*

38 **Introduction:**

39 The mathematical problem related to steady-state water distribution network (WDN) modeling is governed
40 by the two classic balance equations; momentum along pipes and mass (continuity) in internal nodes where the head
41 is unknown. Cross (1936) proposed the first algorithm to solve WDN modeling transforming the mathematical
42 problem to a loop analysis, thus reducing the number of equations during iterative solutions. With the advent of the
43 first computers from the 1960s, many researchers proposed global linearization algorithms, which were characterized
44 by the simultaneous solution of all the equations (Martin and Peters, 1963; Shamir and Howard, 1968; Epp and Fowler,
45 1970; Collins et al., 1978; Isaacs and Mills, 1980; Wood and Rayes, 1981; Carpentier et al., 1987; Todini and Pilati,
46 1988). However, the nodal demands were still considered fixed a priori in the model and relevant WDN modeling
47 approach is designated as demand driven. All the global linearization algorithms iteratively solve a system of linear
48 equations whose size and type depend on the adopted strategy. Of particular note, Todini and Pilati (1988) developed
49 the Global Gradient Algorithm (GGA) that requires the iterative solution of a sparse symmetric system of linear
50 equations whose size is the number of unknown nodal heads. Rossman (2000) developed EPANET for E.P.A
51 (Environmental Protection Agency) US that used GGA as the hydraulic engine, and most current software packages
52 are generally based on this "hydraulic engine".

53 All of the classic hydraulic simulators are created for hydraulic verification, rather than to support
54 management decisions, and for this reason they are based on the assumption of fixed demands at nodes of the water
55 supply network and are called demand-driven, i.e., the pressures calculated at the nodes are "driven by the demand
56 fixed at the nodes". Therefore, during the 1980s, researchers started to investigate the dependence of demand on
57 system pressure, initially by Bhave (1981) and later by Germanopoulos (1985), who combined a leakage term with
58 pressure-dependent customer-demands. Similar head-demand models were soon proposed and, in particular, the
59 generic pressure-demand model for controlled outlets, suggested by Wagner et al. (1988), is considered the most
60 feasible to predict WDN pressure-deficient conditions with respect to customer water requests (Gupta and Bhave,
61 1996). However, although Wagner's pressure-demand relationship for customer-demands is hydraulically consistent,
62 it is not everywhere differentiable (Ackley et al., 2001); thus, several methods were developed to assure the
63 differentiability of pressure-demand relationships (Tucciarelli et al., 1999; Tanyimboh et al., 2001; Tanyimboh and
64 Templeman, 2004). For the same reason, Giustolisi et al. (2008a, b) introduced an adaptive over-relaxation parameter
65 to pressure-driven analysis within GGA and Piller and van Zyl (2007, 2009) developed a pressure-driven WDN model
66 using the "content" and "co-content" proposed by Collins et al. (1978).

67 Progressive urban development has produced increasingly large, complex, and age-old networks, implying
68 that management needs with respect to water losses, reliability, water quality, energy optimization, rehabilitation, etc.
69 The need for analyzing possible pressure-deficit scenarios showed that the classic DDA of EPANET or EPANET like
70 engine are not suitable to support management decisions. Therefore, it was necessary introducing hydraulic simulation
71 capable of evaluating the "actual" demand that can be provided to users when pressures are lower than the minimum
72 pressures for correct service or the leakages outflows. The nodal demands of the advanced hydraulic simulations
73 depend on pressure, then they perform pressure-driven analyses (PDA) as opposite to demand-driven analysis (DDA)
74 of classic hydraulic simulation.

75 Giustolisi et al. (2008) developed the representation of the volumetric water losses demand component, as a
76 function of pressures and deterioration, for each individual pipe. In this way, the accuracy of hydraulic calculations is
77 preserved without losing information at the level of individual pipes. Also, Giustolisi et al. (2014) proposed the
78 demand modeling accounts for local storages supplying water to customers, i.e., nodal demands depending on the
79 filling/emptying process of the local storage, the orifice control type and the customer required demand varying over

80 time. Such local water storage volumes are actually very common in those countries where water supply is intermittent
81 and not reliable. In fact, the use of local tanks, also known as private tanks, has even become mandatory in some
82 regions of the Middle East, such as the UAE. In addition, there are some regions, e.g., in Southern Italy, where private
83 water distribution systems are traditionally fed by private inline water storage whose filling/emptying processes are
84 likely to affect overall system behavior. Some examples are the filling process of inline tanks in intermittent
85 distributions (Criminisi et al., 2009; De Marchis et al., 2011) or after a pressure-deficient occurrence the prediction of
86 the actual supplied customer-demands accounting for the existence of inline tanks. Recently, De Marchis et al. (2018)
87 integrated the private tanks using the orifice area to show the pressure variation with flow in their practical experiment.

88 Whilst some research has been undertaken into the behavior simulation of local tanks in the network, very
89 few of them have focused on the impacts of different tank parameters on the overall network model. Parameters such
90 as orifice and volume size can significantly change the performance of the overall system in terms of carbon footprint
91 and pressure. Therefore, the selected parameters need to be set at their optimum value using reliability indicators.

92 At the component level, the reliability of failure is estimated by determining the failure that occurs during a
93 specified time interval, using a probability density function determined from historical failure data (Liserra, T et al.,
94 2014). Nodal reliability indicators often investigate the performance of nodal junctions based on the level of service
95 in terms of both quantity and quality. These reliability indicators are based on the total demand satisfaction at junction,
96 the water quality or pressure at the nodes (Gargano and Pianese 2000; Tanyimboh et al. 2001), and they are often used
97 to analyze the impact of different parameters on the whole network. For example, Martinez-Rodriguez et al., (2011)
98 used network demand reliability indicators to evaluate the network performance using the water flow supplied to the
99 overall demand. These values of the indicators could also be extended to compare the quality and pressure in the entire
100 network. Then, behavior Simulation technique by McMahon et al., (2006) was to determine the reliability of water
101 supply in presence of tanks by using mass balance technique such as time and volume-based reliability. Time based
102 reliability is the ratio between the total number of occasions in which the full demand was met to the number of time
103 periods in the simulation period. The Volume based reliability is the ratio of the total amount of water actually supplied
104 to the total amount demanded. The weightings presented by these indicators allows assessment of the performance of
105 the network under various configurations of local storage tanks (different orifice and volume sizes). However, the use

106 of reliability in this case would be limited to time and volume-based reliability; these indicators can reflect the
 107 performance of the tank parameters using mass balance techniques.

108 Since, the classical modelling approach does not allow assessment of the reliability of local tanks (as they
 109 are ignored), leading to possible insufficient or oversized design (Cobacho *et al.*, 2008; Criminisi *et al.*, 2009; De
 110 Marchis *et al.*, 2011; De Marchis, Freni and Milici, 2016, 2018; Mohamed *et al.*, 2019). Insufficient design can lead
 111 to failure where the tank cannot provide the required consumer demand and oversized design can alternatively increase
 112 the cost and deteriorate the water quality. Hence, the purpose of the work reported herein is to demonstrate how
 113 advanced hydraulic modeling of WDN can be used to investigate the impact of local tank parameters (orifice and
 114 volume size) on reliability, pressure, and carbon footprint, thus supporting WDN management actions.

115 **Methodology:**

116 When modelling local storage, the flow through the tank's inlet depends upon orifice diameter, available
 117 storage, orifice level, available pressure in the network, coefficient of discharge and pattern of consumers' water
 118 demand. They are modelled as free orifice, by using PDA, whose size is controlled by storage volume. This is because
 119 the node of the network is connected to the orifice of the local tank and not directly to the consumer as assumed during
 120 the design phase of the network, even though the capacity-demand function of the reservoir is affected by the flow to
 121 the tank which is itself affected by pressure in the network and the orifice diameter of the inlet. This leads to a change
 122 in the simulation process in the network.

123 **Steady-state hydraulic modelling and local storages**

124 For simulation of WDN, the system of momentum and continuity equations at pipes and internal nodes,
 125 respectively, can be written in the matrix form as in Equation 1 (Giustolisi *et al.* 2012),

$$\begin{aligned}
 \mathbf{A}_{pp}(t)\mathbf{Q}_p(t) + \mathbf{A}_{pn}\mathbf{H}_n(t) &= -\mathbf{A}_{p0}\mathbf{H}_0(t) \\
 \mathbf{A}_{np}\mathbf{Q}_p(t) - \frac{\mathbf{V}_n(t, \mathbf{H}_n(t))}{\Delta T} &= \mathbf{0}_n
 \end{aligned}
 \tag{1}$$

127 For each simulation snapshot t , \mathbf{Q}_p is the column vector of unknown pipe flow rates; \mathbf{H}_n is the column vector
 128 of unknown nodal heads; \mathbf{H}_0 is the column vector of known nodal heads and \mathbf{V}_n is the column vector of volume
 129 outflows during ΔT lumped at nodes. \mathbf{A}_{pn} , \mathbf{A}_{np} and \mathbf{A}_{p0} are topological incidence sub-matrices of the general topological
 130 matrix, link-node, of the network. The subscript p and n indicate the dependence of the matrices and vectors on the

131 number of pipes and nodes (related to unknown heads), while the subscript “0” refers to the number of reservoirs
 132 (known heads). The second part of Equation (1) represents mass-balance at model nodes and $\mathbf{V}_n = \mathbf{d}_n \cdot \Delta T$ where \mathbf{d}_n are
 133 the stationary demand components (Giustolisi and Walski, 2012) in ΔT generally depending on pressure through \mathbf{H}_n .
 134 Equation (2) explicitly reports all demand components that are included in \mathbf{V}_n .

$$135 \quad \mathbf{V}_n(t, \mathbf{H}_n(t)) = \mathbf{V}_n^{cons}(t, \mathbf{H}_n(t)) + \mathbf{V}_n^{priv-tank}(t, \mathbf{H}_n(t)) + \mathbf{V}_n^{orif}(t, \mathbf{H}_n(t)) + \mathbf{V}_n^{tank}(t, \mathbf{H}_n(t)) + \mathbf{V}_n^{leak}(t, \mathbf{H}_n(t))$$

136 (2)

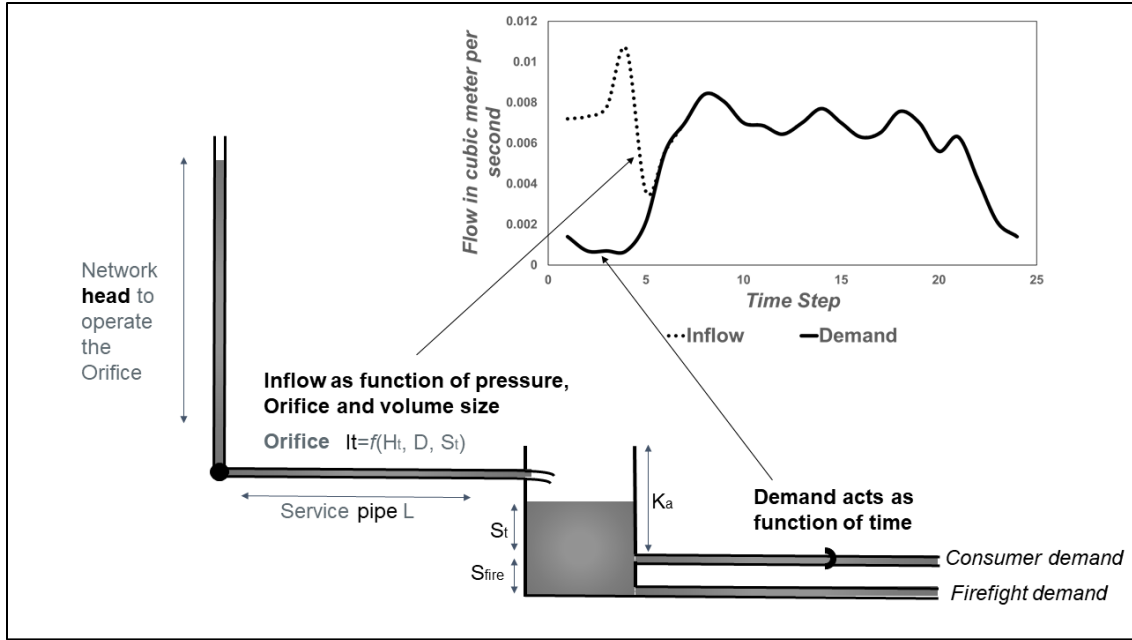
137 Where $\mathbf{V}_n^{cons}(t, \mathbf{H}_n(t))$ is the water demand supplied to *consumers* directly connected to the water network: if
 138 nodal pressure is higher than the minimum value to supply service to consumers (i.e. by contract) it equals the
 139 *statistical* water requests while, in case of pressure-deficient conditions, it returns the water volume supplied to
 140 consumers consistently with Torricelli law.

141 $\mathbf{V}_n^{priv-tank}(t, \mathbf{H}_n(t))$ represents the volume of water feeding private storage tanks in ΔT , as a in Giustolisi et al.
 142 (2014). Such function depends on tank filling conditions at the beginning of the simulation time step and on pressure
 143 at n^{th} node. Thus, filling/emptying of private tanks affects WDN hydraulic status, especially in water shortage
 144 conditions (e.g. De Marchis et al., 2018).

145 $\mathbf{V}_n^{orif}(t, \mathbf{H}_n(t))$ is the water volume from uncontrolled free orifices, e.g. from hydrants. The outflow coefficient
 146 of uncontrolled orifices is known for manufactured devices (e.g., hydrants, sprinkler systems), while it is unknown
 147 and might be variable with pressure for orifices representing pipe bursts.

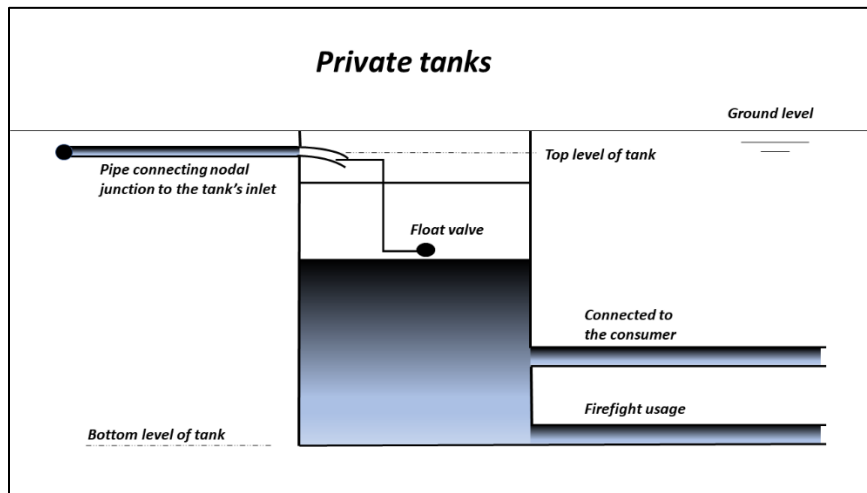
148 $\mathbf{V}_n^{tank}(t, \mathbf{H}_n(t))$ represents the water volume to/from *tanks* whose consistent and stable simulation is affected
 149 by the global water balance in the system (Giustolisi et al. 2012). It must remark that \mathbf{V}_n^{tank} refers to urban tank in
 150 WDN, not private tanks.

151 $\mathbf{V}_n^{leak}(t, \mathbf{H}_n(t))$ represents leakage volume due to pressure-dependent outflows from holes, cracks, joints and
 152 fittings. Few models are available in the literature to represent pressure-leakage demand component \mathbf{V}_n^{leak} , e.g.
 153 Germanopoulos (1985), Germanopoulos and Jowitt (1989), May, (1994), Giustolisi, O. et al., (2008a) and, Van Zyl
 154 and Cassa, (2015).



156 *Fig. 1 Actual scenario with private tanks, modified after (Giustolisi et al., 2014)*

157 Focusing on the component $V_n^{priv-tank}$, the simulation of private storages cannot be performed using DDA
 158 because when the local tank is not completely filled, a process of filling/emptying occurs, and the inlet is a free orifice
 159 whose size is controlled by tank volume as shown in Fig. 1. In other words, private tank simulation involves DDA
 160 when the tank is filled during the snapshot ΔT , i.e., it starts filled and the discharge from the free orifice equals the
 161 required demand, otherwise PDA is mandatory. A schematic of private local tank is shown in Fig. 2.



163 *Fig. 2 Layout of a common underground private tank*

164 **Sample networks**

165 In this study, the data of a WDN was collected from *Walski et al., (2003)* and a real-time network from Dubai,
166 UAE. For each network, every single attribute including the nodal data, base water demand, pipe characteristics, valve
167 settings, property of water sources, additional storage(s) data, pump curve(s), type(s) and scheduling were used. From
168 these attributes, some of the missing information for private tanks, such as the volume and orifice diameter(s), have
169 been initially assumed based on the given standards by Dubai Electricity and Water Authority (DEWA) and general
170 practices from the local developers in UAE. In total, two sample networks were built to show the difference in the
171 reliability analysis of private tanks at each case. The initial assumed orifice diameter was taken as 2cm (minimum
172 specification) and the volume size was assumed to be equivalent to 6 hours of average daily water use, i.e. retention
173 time of 6 hours. The initial level of the tank was set to empty to account for the worst-case scenario. Furthermore, as
174 the minimum pressure to achieve the required demand varies between 10m to 15m based on the practices from
175 different countries, it was taken as 12.5m in this case.

176 Network 1(Fig. 3): WDN containing two variable tanks and a single reservoir connected to nodal junctions
177 of the network by a single pump. The outline of the network ensures that there would be enough pressure to supply
178 the required demand using pumps and variable tanks (*Walski et al., 2003*). This network is used to showcase, in detail,
179 the effect of changing orifice and volume size of private tanks using reliability indicators. Furthermore, it also shows
180 the changes in pressure and carbon footprint with increasing the orifice and volume sizes.

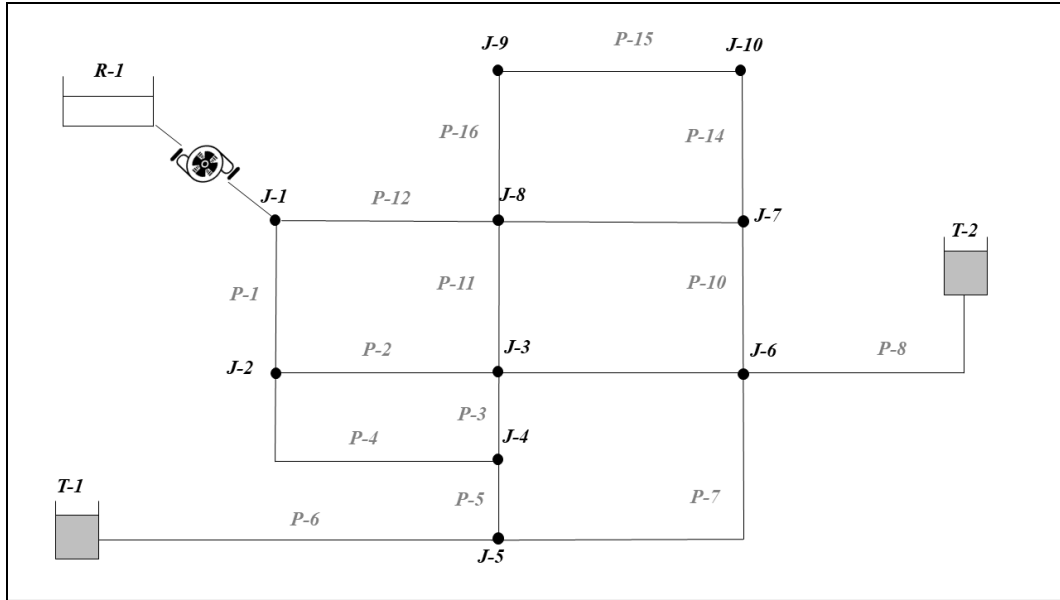


Fig. 3 Schematic of Network 1 (Walski et al., 2003)

182

183 Network 2 (Fig. 4): The schematic of the WDN represents a real-time network based on the area of Dubai
 184 Silicon Oasis (DSO) network in Dubai, UAE. The network model was built based on the approved master plan for the
 185 development of this community. The system was built to supply a total of 45000m³ per day to the estimated population
 186 of more than 150,000 living/or working in DSO, but in reality, the current population is far lower as the area is still
 187 growing. Hence, the current real time network is functioning partly where some of the pipes in the network are not
 188 operational, and the running time of the pump is limited. Therefore, the model was designed from the pre-approved
 189 plan that will eventually be implemented in the real network once the entire area is populated.

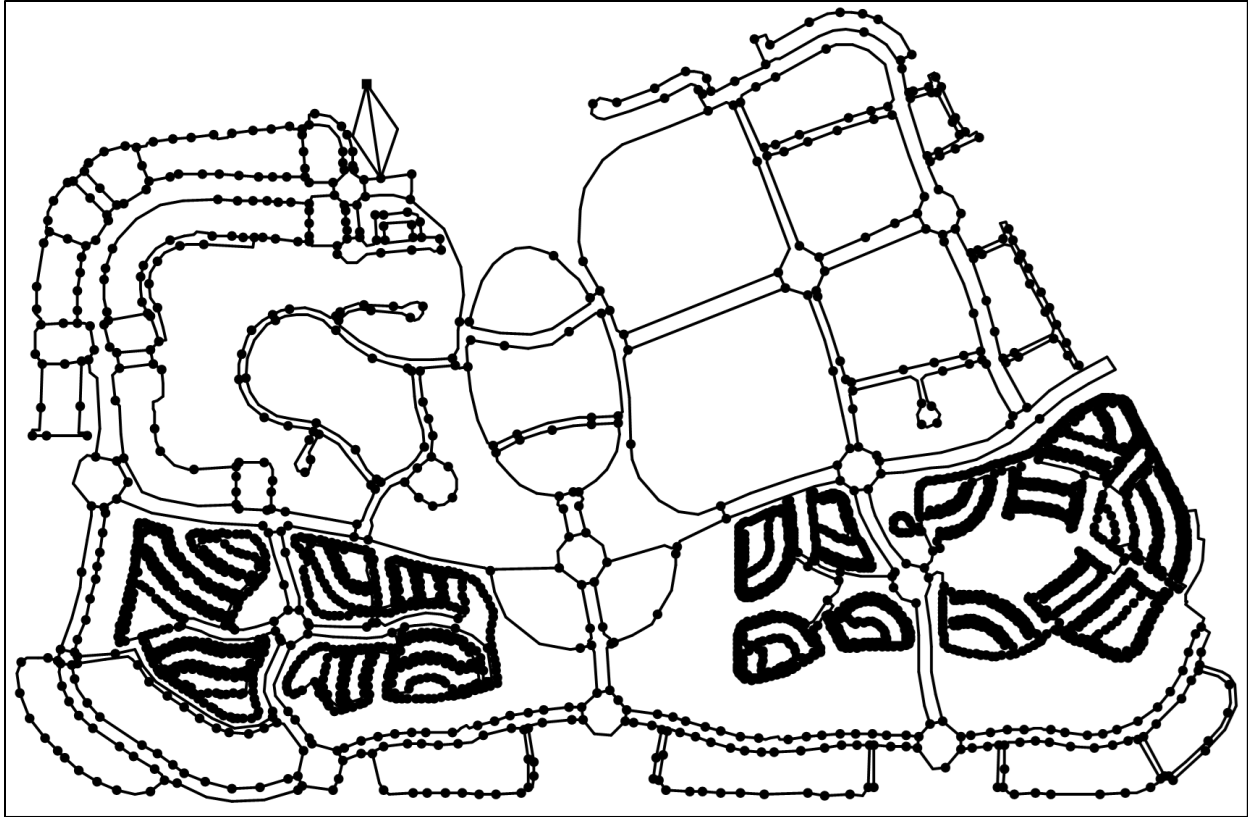


Fig. 4 Schematic of Network 2

191

192

193

194

195

196

197

198

199

Generally, Network 2 is a branched network, containing a total of 2550 junctions and 2750 pipe links. The water is supplied using a single source reservoir connected via three pumps running in parallel. Pipe diameters range between 150mm to 900mm, while the daily demand per capita is close to 550 liters per day. The estimated number of users is close to 165,000 capita. The elevation of the area varies, with few areas higher than the reservoir head of 30m. The nodal characteristics of the network varies as the area itself consists of a range of different residential buildings, villas, commercial buildings, educational schools, governmental offices, and hospitals. The purpose of this case study is to validate the theory based on larger real networks, with a greater number of nodes and junction. Furthermore, the analysis uses flow paths to showcase the effect on pressure by changing the properties of few junction tank nodes.

200

201

202

Assuming that the present analysis refers to design stage, water losses (pipe leakages) from WDN are neglected. Nonetheless, the analyses reported in this paper apply to support management decision on aged systems with known water losses, for which the parameters of the leakage model can be estimated.

203 **Analysis and working of the simulation:**

204 The adopted hydraulic model (i.e., Giustolisi et al., 2014) implements private tanks by using a pressure-
 205 demand function which accounts for the filling/emptying process based on orifice diameter varying with stored
 206 volume in each tank.

207 In case the orifice of the tank has two states only, closed or fully open (ON/OFF control), $C(t)$ is constant in
 208 ΔT if V_i^{max} is not reached. Thus, the mass balance in Equation (1) allows writing:

$$209 \quad V(t + \Delta T) = d^{fill} \Delta T - d^{act} \Delta T + V(t) \text{ with } d^{fill}(t) = C^{max} \sqrt{P(t) - \Delta Z^{orif}} \quad (3)$$

210 where $d^{fill}(t)$ = average flow rate filling the tank during ΔT , $P(t)$ is the head pressure at the time t , ΔZ^{orif} is
 211 the elevation of the orifice inlet from the ground and C^{max} = maximum outflow coefficient of the orifice. The C^{max} was
 212 modified to incorporate the orifice diameter during the simulation and was represented by:

$$213 \quad C^{max} = \frac{C_D \pi d^2 \sqrt{2g}}{4} \quad (4)$$

214 Where C_d is the coefficient of discharge, d is the diameter and g is acceleration due to gravity. The following
 215 formulations are adopted for $d_i^{fill}(t)$ and the delivered customer demand $d_i^{act}(t)$ at the i^{th} node (Giustolisi et al., 2014):

$$216 \quad d_i^{fill}(P_i(t), V_i(t)) = \begin{cases} d_i^{act}(t) + \frac{V_i^{max} - V_i(t)}{\Delta T} & V_i(t + \Delta T) > V_i^{max} \\ C_i^{max} \sqrt{P_i(t) - \Delta Z^{orif}} & V_i(t + \Delta T) \leq V_i^{max} \end{cases} \quad (5)$$

$$217 \quad d_i^{act}(P_i(t), V_i(t)) = \begin{cases} d_i^{req, hum}(t) & V_i(t + \Delta T) > V_i^{max} \\ C_i^{max} \sqrt{P_i(t) - \Delta Z^{orif}} + \frac{V_i(t)}{\Delta T} & V_i(t + \Delta T) \leq V_i^{max} \end{cases} \quad (6)$$

218 In the case of a tank becoming empty during Δt , the assumption $V(t + \Delta T) = 0$ holds and

$$219 \quad d_i^{act}(t) = C_i^{max} \sqrt{P_i(t) - \Delta Z^{orif}} + \frac{V_i(t)}{\Delta T} \quad (7)$$

220 where $d_i^{act}(t)$ = actual average demand supplied to customers during ΔT . This means that the tank completely
 221 empties during ΔT , although the orifice is fully opened, because the inflow summed to the initial water volume is
 222 insufficient to satisfy the customer water requests.

223 In the case of a tank becoming completely full during ΔT , the assumption $V_i(t+\Delta T) = V_i^{max}$ holds and, it is
 224 possible to assume a fixed flow rate filling the tank over ΔT given by:

$$225 \quad C_i^{max} \sqrt{P_i(t) - \Delta z^{orif}} \geq d_i^{act}(t) + \frac{V_i^{max} - V_i(t)}{\Delta T} \Rightarrow d_i^{fill}(t) = d_i^{act}(t) + \frac{V_i^{max} - V_i(t)}{\Delta T} \quad (8)$$

226 In this case the customers' demand at the i^{th} node is satisfied and $d_i^{act}(t) = d_i^{req,hum}(t)$. Where $d_i^{req,hum}(t)$ is the
 227 required demand by the consumer during ΔT . It is taken from the water demand profile at specific time interval.

228 The above detailed explanation of the demand model for private tanks at the i^{th} node can be extended to any
 229 kind of control (Giustolisi et al., 2014). Hence, the advanced hydraulic model accounting for local tanks, allows
 230 harmonizing different design parameters (orifice diameter, orifice level and volume of local tanks) by using reliability
 231 analysis.

232 Reliable design can be achieved with different volume and orifice diameter combinations that satisfy the
 233 consumer demand without hydraulic failure. The time and volume-based reliability indicators could be calculated
 234 based on the result of the simulation by using Equation 9-12 (Adeloye et al., 2017).

$$235 \quad R_t = 1 - \frac{\sum_{t=1}^N f_t}{N} \quad (9)$$

$$236 \quad R_v = 1 - \frac{\sum_{t=1}^N f_t (d_i^{req,hum}(t) - d_i^{act}(t))}{\sum_{t=1}^N d_i^{req,hum}(t)} \quad (10)$$

$$237 \quad f_t = \begin{cases} 1, & \text{if } d_i^{act}(t) < d_i^{req,hum}(t) \\ 0, & \text{otherwise} \end{cases} \quad (11)$$

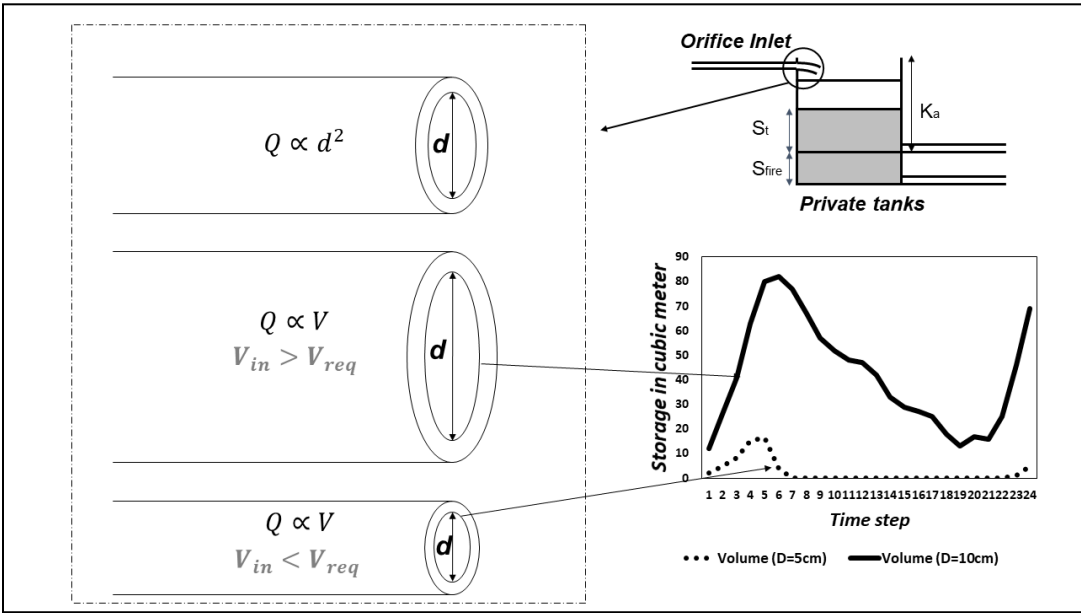
$$238 \quad d_i^{act}(t) = \begin{cases} d_i^{fill}(t) + V(t), & \text{if } V(t) + d_i^{fill}(t)\Delta t \leq \Delta t d_i^{req,hum}(t) \\ d_i^{req,hum}(t), & \text{if } d_i^{req,hum}(t)\Delta t \leq V(t) + d_i^{fill}(t)\Delta t \leq K_a \end{cases}$$

Where $V(t)$ is initial storage

239 (12)

240 where N is the total number of time periods, i.e., time steps of the extended period simulation representing
 241 the typical operating cycle, R_v is the ratio of the total amount of water actually available to the customer and the desired
 242 amount demanded, and R_t is the ratio between the total number of time steps in which the full demand was met to the
 243 number of time steps in the extended period simulation. The required reliability to achieve the consumer consumption

244 is equal to 1 for each local tank. Therefore, the sizing of the orifice is an important tool as it can restrict the incoming
 245 flow to the tank. For example, if the diameter of the opening is too small then the local tank might not be able to
 246 achieve the required reliability even if there is enough pressure to satisfy demand as shown in Fig. 5.



247

248 *Fig. 5 Impacts of orifice sizing on Volume (V is the volume, Q is the flow and d is diameter)*

249

Carbon footprint:

250

251 Carbon footprint depends on the power required by the pump that is operating the network. Often power is
 252 calculated by the flow, total head, density of the water being pumped, mechanical efficiency and acceleration due to
 253 gravity (Walski, T., 2003).

253

$$P = \frac{\rho g H Q}{\eta} \tag{13}$$

254

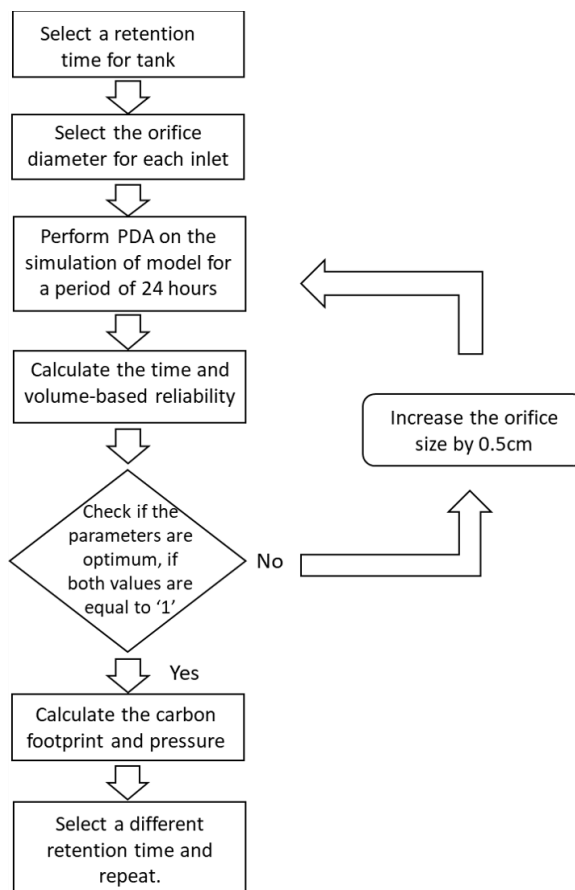
255 where P stands for power in kW, H is total head (suction head-discharge head) in m, Q represent the
 256 discharged flow rate m³/s, ρ refers to the density of water being discharged, and η is the efficiency factor. A simple
 257 factor is applied to the obtained power of the pump(s) that differs from country to country to obtain the carbon
 258 footprint. A factor of 0.43 was applied on the overall total power obtained from the pump to obtain the carbon footprint.

258

259 Hence, the investigation itself would be a trial-and-error approach to achieve the required reliability of 1 by
 the following steps:

- 260 1. Obtaining the demand data, volume and orifice diameter of the tank based on the codes and selecting the time
 261 period of the simulation,
 262 2. Perform the simulation which will give the number of failures by using advanced hydraulic modelling
 263 encompassing Equations 1-8,
 264 3. Calculate the time and volume-based reliability based on equation 9-12 for multiple orifice and volume size,
 265 4. The optimum size is chosen once the lowest orifice and volume parameters achieves the required reliability,
 266 5. Steps 1 to 4 are repeated with different orifice inlet level to obtain the best parameters in terms of low carbon
 267 footprint and pressure.

268 The above steps are summarized in a flow chart in Fig. 6. Therefore, the idea is to investigate the reliability
 269 of the tanks with different retention times and orifice diameter, without changing the geometry of the network.



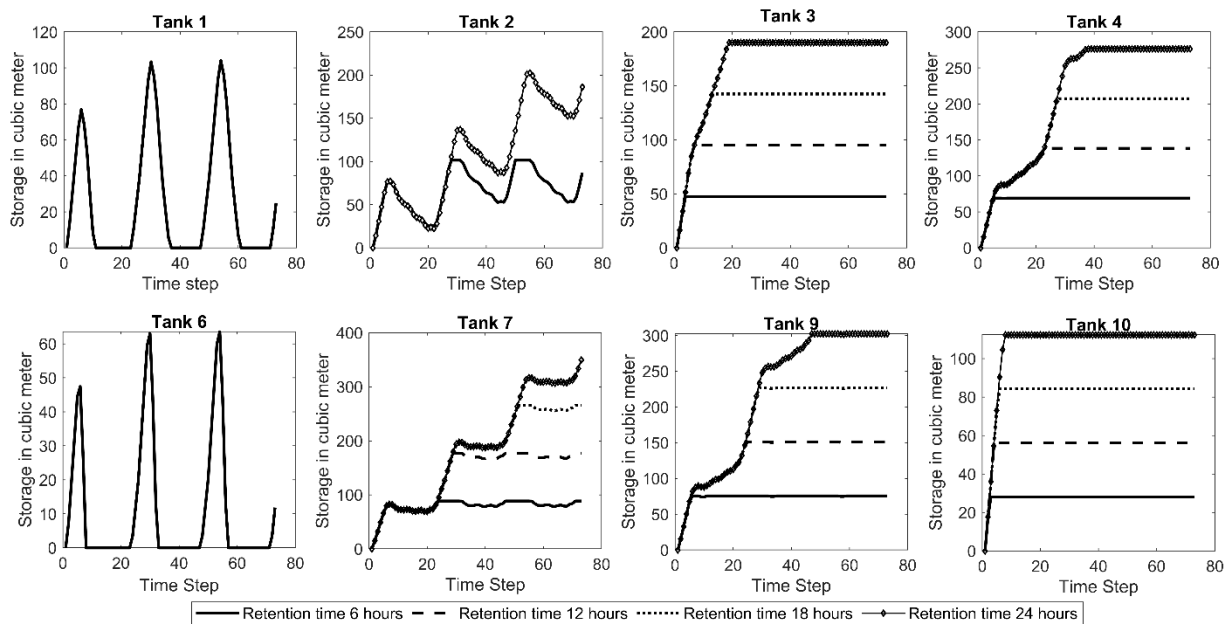
271

Figure 6 Flow chart of the entire process

272 **Results and Discussion:**

273 **Network 1: WDN containing two tanks and single pump supplied from a source.**

274 For network 1, Fig. 7 showcases storage at each time interval for every tank in the network. The comparison
 275 between each plot is drawn based on different retention times to show the impact of volume capacity. The area of
 276 success and failure is based on the storage level at different times; where reaching to zero instantly means that the
 277 tank is unable to satisfy the consumer demand.

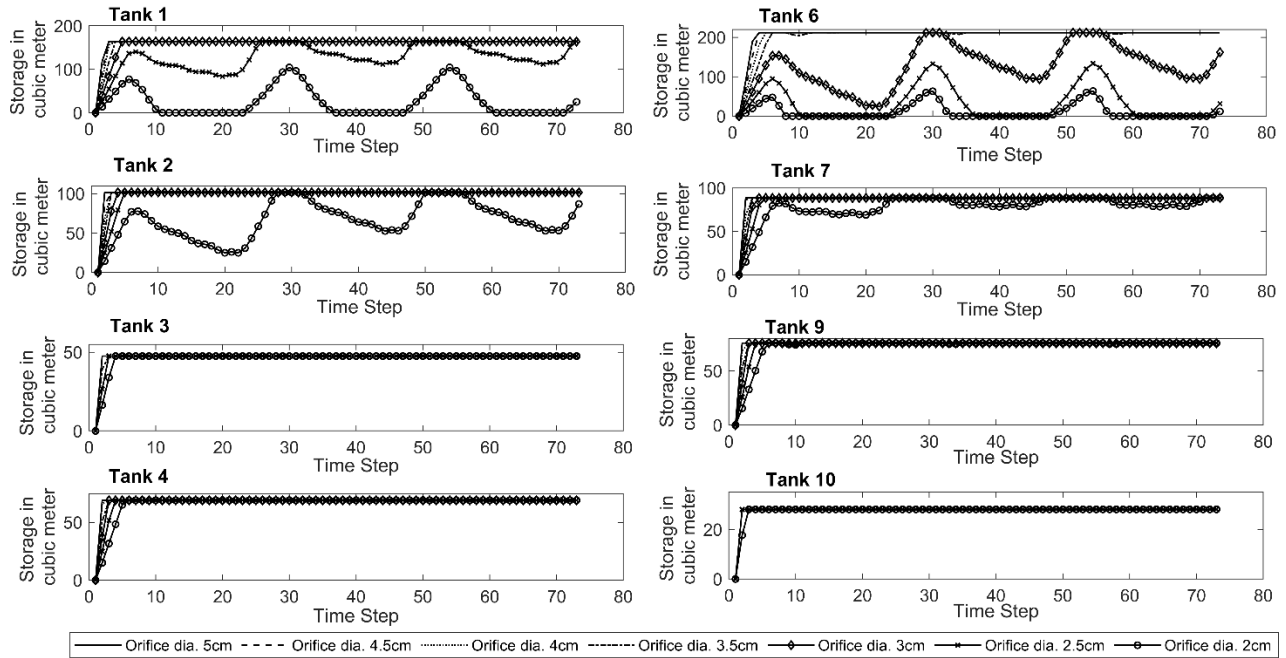


279 *Fig. 7 Simulated storage for different retention times (orifice diameter constant at 2cm)*

280 One of the key things noted in Fig.7 is that increasing the volume size does not always lead to improvement
 281 in reliability. In fact, it has been seen that changing the retention time for tank '1' and '6' did not made any significant
 282 impact on the reliability of the tank; this is because the orifice diameter of the tank is too small to fulfill the consumer
 283 demand at relevant time periods. This is also justified as the base demand at the nodal junction for each tank is
 284 relatively higher than at any other nodes. On the contrary, increasing the volume size for other tanks increases the
 285 storage capacity as the tank regularly fills without depleting as seen for tank '10'. However, the common concern with
 286 large tanks is that the water quality drops as water stays in the tank for too long without being renewed. It indicates
 287 that the volume of the private tanks is larger than required which can cause water stagnation. This could be improved
 288 by decreasing or restricting the orifice diameter which changes the actual inflow coming into the tank. Therefore, to

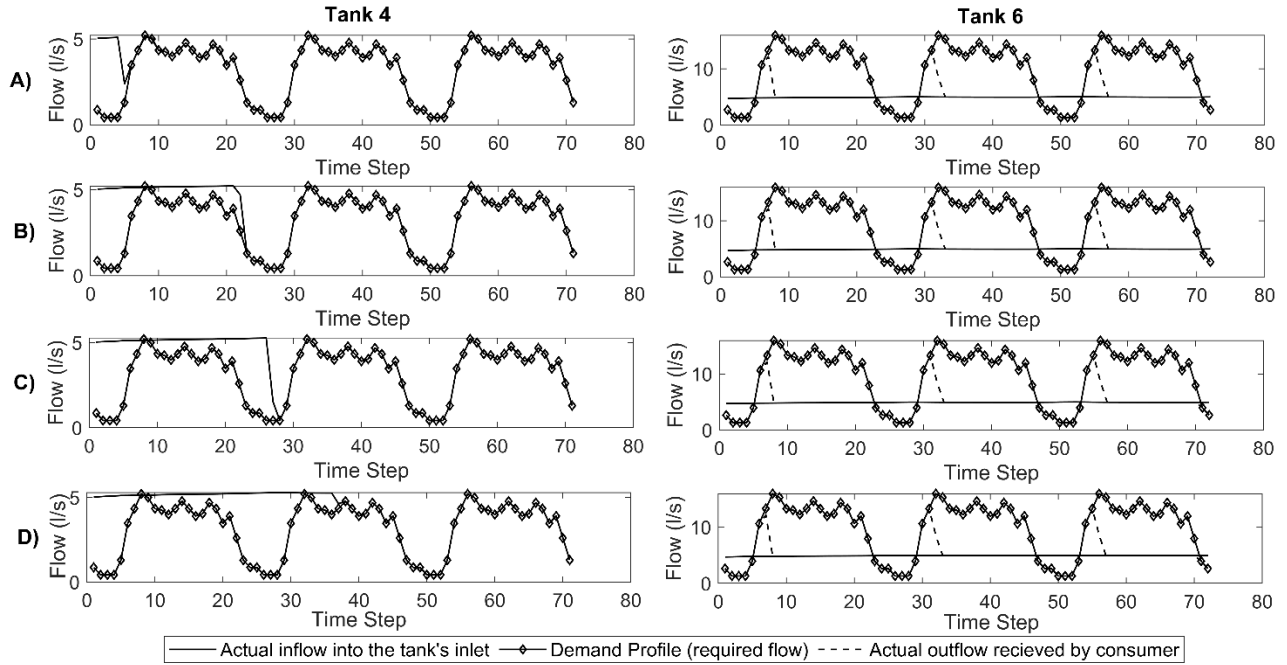
289 reflect on the impact of the orifice diameter, simulations were repeated while keeping the retention time constant and
 290 changing the orifice diameter for every local tank in the network.

291



293 *Fig. 8 Simulated storage for different orifice diameter of the private tanks (Volume size equivalent at*
 294 *retention time of 6 hours)*

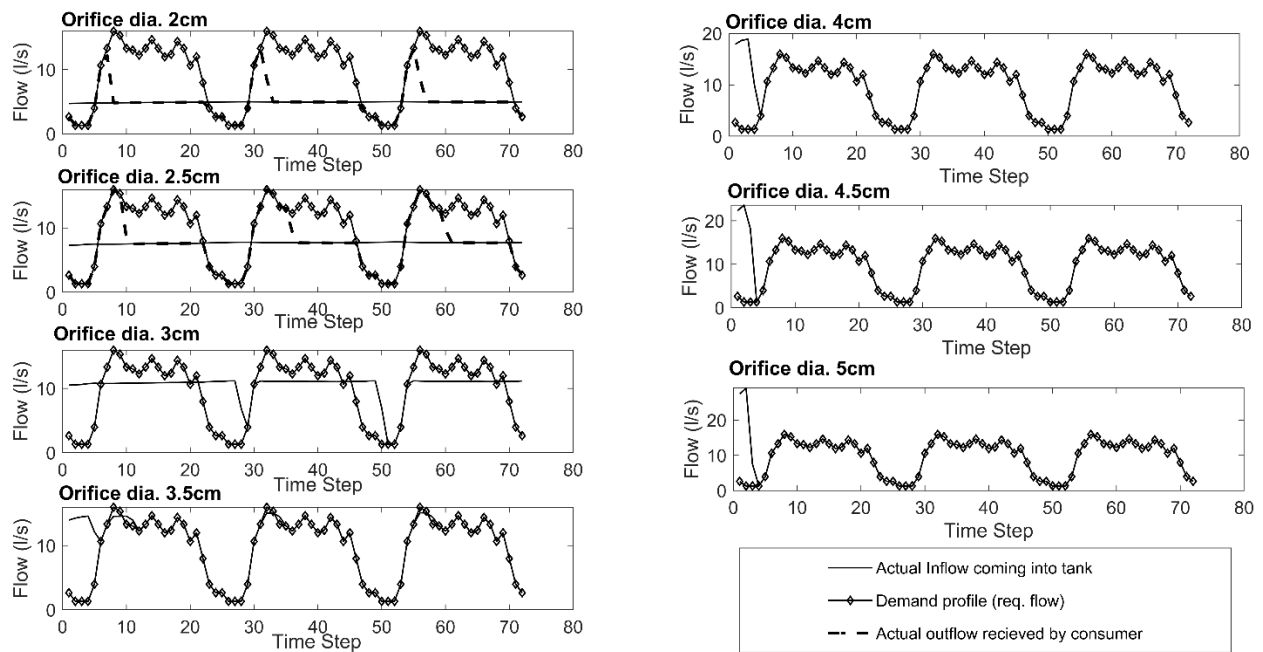
295 The results in Fig. 8 show that increasing the orifice diameter for tank ‘1’ and ‘6’ allows them to achieve the
 296 required demand. Based on the storage level, it is observed that shifting from 2cm to 2.5cm allows tank ‘1’ to fulfill
 297 the demand without being completely empty (tank failure). While for tank ‘6’, the orifice diameter of 3cm is sufficient
 298 to satisfy the user’s water requirement. In fact, this also shows that fewer changes in orifice diameter are as impactful
 299 as increasing tank volume. Furthermore, for the remaining tanks, increasing the orifice diameter allows them to reach
 300 their capacity in a much shorter time as the inflow increases from the tank’s inlet. To illustrate this effect in detail,
 301 Fig. 9 and 10 shows the comparison of inflow with outflow for different retention times and orifice diameter,
 302 respectively.



304 Fig. 9 Simulated flow for tanks 4 and 6 with retention time of a) 6 hours b) 12 hours c) 18 hours and d) 24 hours

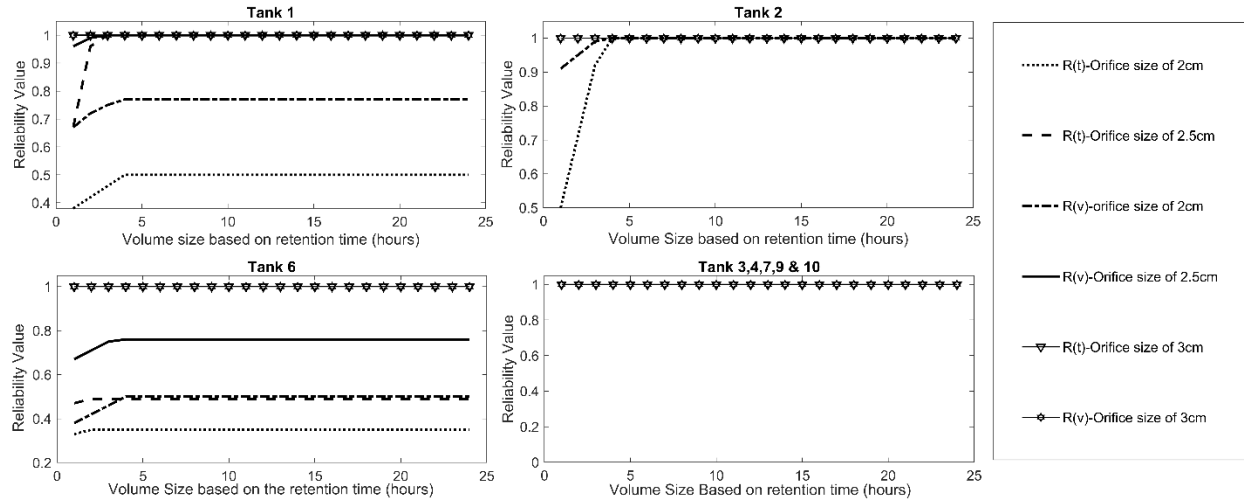
305 In Fig. 9, the actual inflow is referred as the incoming flow to the tank's inlet (i.e., $d^{in}(t)$). During the periods
306 when tank is close to full, the actual inflow curve becomes similar to the desired demand. The desired demand is the
307 maximum required water consumption obtained from the Water Demand Profile. Finally, the actual outflow is referred
308 as the outgoing flow coming out from the tank. The actual outflow will be equal to the desired demand unless there is
309 insufficient flow coming into an empty tank. Any gap between the desired demand and outflow would be indicated as
310 tank failure. The area between the outflow and desired demand is taken as the required storage to prevent tank failure.
311 Moreover, the private tank fills up when the actual inflow is higher than the desired demand and begins to empty when
312 the desired demand is more than the inflow. With above description laid out, the results in Fig. 9 take in account of
313 different retention times for two tanks '4' and '6', with orifice diameter kept constant at 2cm. As seen before, tank '4'
314 was able to satisfy the demand as the inflow in the tank's inlet is higher than the required consumption profile. With
315 lower retention time (6 hours), the tank can reach its full capacity as the inflow and outflow curves become similar
316 from the time 6hrs, due to the closure of inlet. Increasing the retention time further, means the inflow curve takes more
317 time to become equivalent to the water demand curve (tank is close to full) as the water keeps on filling the tank. In
318 fact, when using a very high retention time of 24 hours, it can take up to 40 hours for the tank to reach its maximum
319 capacity. However, for tank '6', increasing the retention time has no effect on the inflow as the control is the restricted

320 orifice diameter. Hence, the outflow curve does not coincide with the required demand indicating that the tank is
 321 empty.



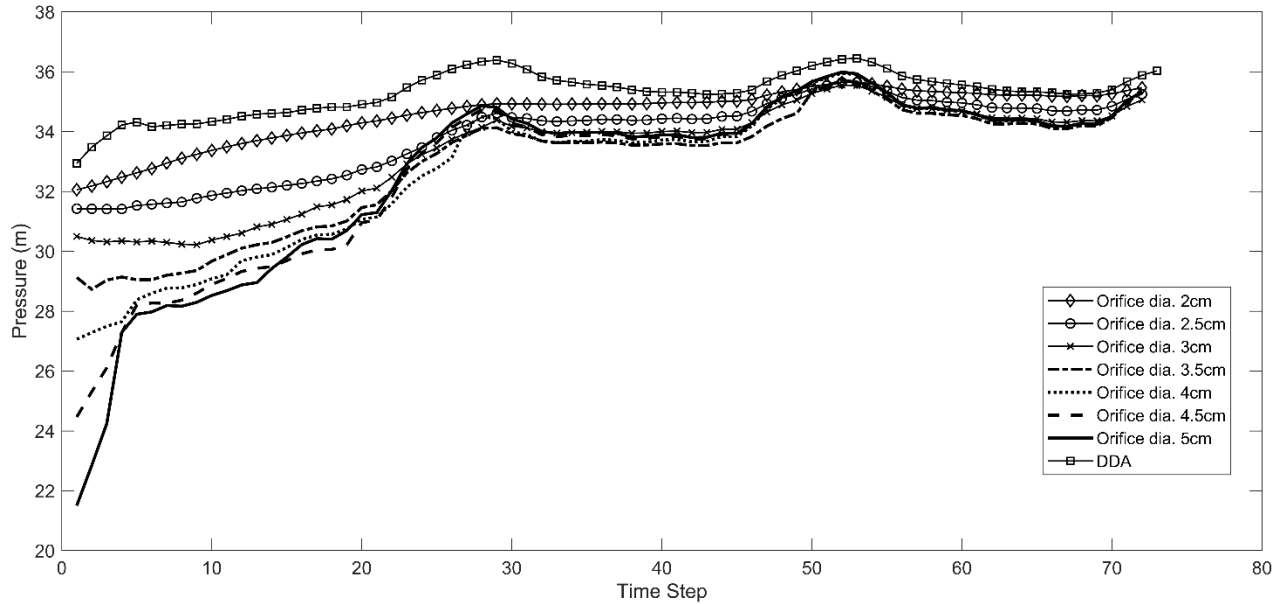
323 *Fig. 10 simulated flow for tank 6 with changing orifice diameters*

324 In Fig. 10, tank ‘6’ with increased orifice diameters; the results show that the inflow curve increased as the
 325 orifice diameter increased. The incoming flow (actual inflow) is increased when the orifice diameter changed from
 326 2cm to 2.5cm, gradually reducing the required storage, area between the desired demand and outgoing flow. Yet, the
 327 tank fails due to insufficient storage to satisfy the desired demand. Hence, when the diameter is increased further to
 328 3cm, the tank can fulfil the required demand (no gap between desired demand and outflow). The tank also reaches it
 329 maximum capacity as indicated from the inflow curve for the orifice diameter of 3cm at time 30 and 50 hours. The
 330 inflow drops and becomes equal to the demand at those times, which shows that the pressure has dropped due to
 331 closure of the orifice. Additionally, any increase in the orifice diameter above 3cm would be unnecessary and might
 332 reduce the pressure at downstream nodes due to increased inflow.



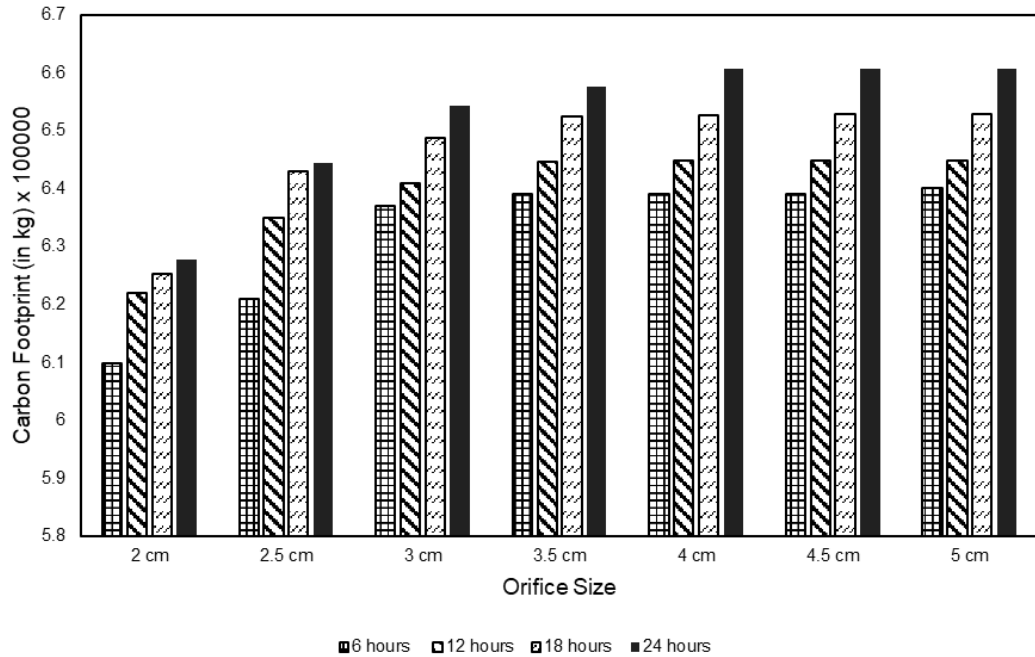
334 *Fig. 11 Reliability analysis for each tank in the network*

335 Finally, Fig. 11 shows volume and time-based reliability indicators for different tank retention time and
 336 orifice diameter. It is also worth noting that both the reliability indicators have variations in their value due to the
 337 difference in outgoing flow and desired demand. The volume-based reliability indicators tend to give more weightage
 338 to the values of partial flow that satisfy a small portion of the demand. On the other hand, the time-based reliability
 339 indicators only analyze performance of the tank based on satisfying the full requirement of the consumer, therefore it
 340 does not give any weightage to partial flows. Their graphical representation in Fig. 11 indicates that the reliability
 341 value increases with higher retention time, to a certain extent, for tanks '1' and '6'. It also shows that none of the
 342 retention times can achieve the required reliability of 1. However, the other tanks are able to achieve their required
 343 reliability with minimal volume sizes and hence, increasing the retention time does not impact the indicators.
 344 Similarly, the reliability indicators show the impact of changing the orifice diameter for different local tanks. For tank
 345 3,4,7,9 and 10, increasing the orifice diameter did not have any impact on the reliability as it is already at maximum.
 346 For tank 1, increasing the orifice diameter just by 0.5cm allows it to reach the required reliability. Finally, for tank
 347 '6', increasing the diameter does increase the reliability value for both indicators, however, it needs to be raised till
 348 3cm to achieve the required reliability.



350 *Fig. 12 Pressure variation with different orifice diameters for tank 6 and from DDA (without the inclusion of tanks)*

351 For every scenario mentioned above, Fig. 12 represents the fluctuation in pressure to show the impact of
 352 changing orifice for tank ‘6’, as similar results were subjected in other tanks. Fig. 12 also contains the pressure pattern
 353 obtained without the integration of local tank (as commonly practiced by engineers) to show the effects of integrating
 354 local tanks. Firstly, it is noted that increasing the orifice diameter, decreases the pressure, as decreasing diameter leads
 355 to an increased inflow which itself results in a higher head loss and hence a lower pressure. Secondly, the result does
 356 indicate that the pressure values, as certain time periods become similar to that of DDA. More commonly, this happens
 357 once all tanks in the network is completely full. For example, the pressure fluctuations of DDA and orifice diameters,
 358 that is above or equal to 3cm are the same which indicates that the tank reaches its full capacity. In fact, increasing
 359 the diameter allows the tanks to be filled up much sooner, therefore, the pressure curve becomes much more similar
 360 to DDA. Lastly, it should be noted that the variation in pressure can differ quite drastically especially if the comparison
 361 is drawn between large and smaller orifice diameters with higher retention times. In fact, the pressure drop of 12m
 362 was noted in this case (when comparing orifice diameter of 2cm and 5cm), which indicates very high head loss without
 363 changing any feature of the network (e.g., pipe hydraulic resistance, pressure control devices).



365 *Fig. 13 Carbon footprint comparison with different orifice and volume size for all tanks*

366 The carbon footprint of any system is directly related to the power utilized by the pumps. Fig. 13 shows the
 367 impact of changing orifice diameter and tank volume on the production of carbon footprint. It shows that the carbon
 368 footprint increases with orifice diameter, as the flow rate increases which causes the pumps to utilize more power to
 369 distribute water in the network. The carbon footprint eventually starts to become constant when using large orifices
 370 between 4cm to 5cm (for every retention time), as all tanks remains full in the network model. Similarly, having a
 371 larger retention time increases the carbon footprint as more water is pumped again into the network to fill these large
 372 local tanks. In fact, the carbon footprint differs vastly when comparing the small orifice diameter of 2cm at a low
 373 retention time of 6 hours, with the large orifice diameter of 5cm at a higher retention time of 24 hours.

374 **Network 2: Silicon Oasis network**

375 Table 1 Optimum setting of the orifice and volume size for each type of node

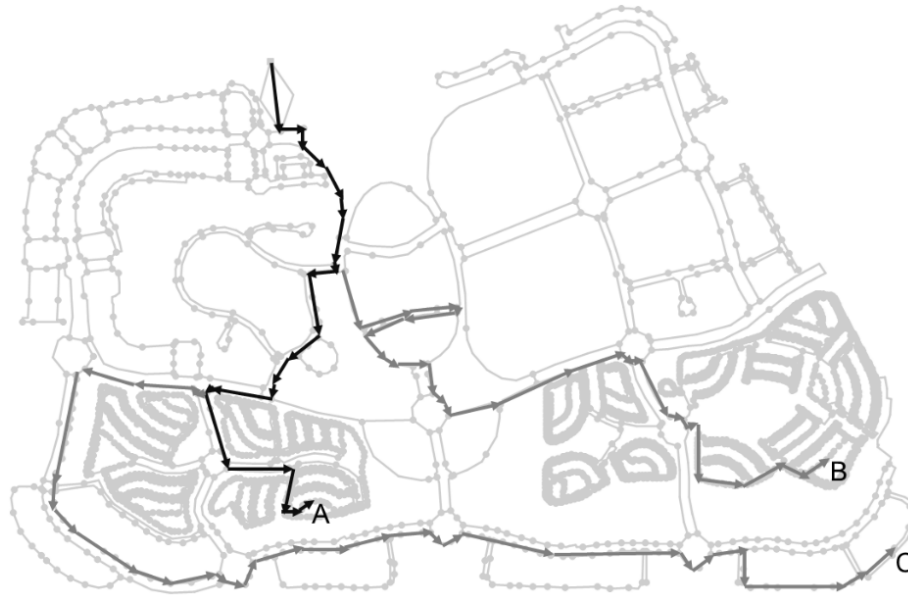
	Percentage of nodes (%)	Demand (m ³ /d)	Optimum Orifice diameter (cm)	Optimum Volume size (in hours)
Villas	58	2-5	2	6
Low-rise buildings	18	50-70	2	6

Medium-rise buildings	9	80-150	2-3	6
High-rise buildings	9	400-650	5	6
Offices	3	90-100	2-2.5	6
Governmental building	1	60	2	6
Schools	1	220	5	6
Hospitals	1	450	5	6

376

377 Table 1 shows the optimum (lowest) orifice diameter and tank volume to achieve a reliability of 1. It should
378 be noted that, due to the high number of the nodal junctions, Table 1 does not include every single node, but rather
379 those with similar characteristics based on their base demand. It also includes the percentage of each nodal type to
380 showcase the characteristic of the network.

381 It is clear that the selection of orifice diameter depends on the base demands as higher orifice diameters are
382 normally chosen for higher demands in the network. In general terms, most of the optimum orifice diameters in this
383 network range between 2-3cm followed by the orifice diameter of 5cm. The optimum tank volume is that to achieve
384 a retention time of 6 hours, for each case signifying the use of smaller tanks.



386

Fig. 14 Flow path A, B and C for the DSO network

387

To add further, the diameter of the orifice is now increased to showcase the impact on a real-time network.

388

In total, 3 flow paths are selected to capture the most significant parts of the network based on the pressure difference,

389

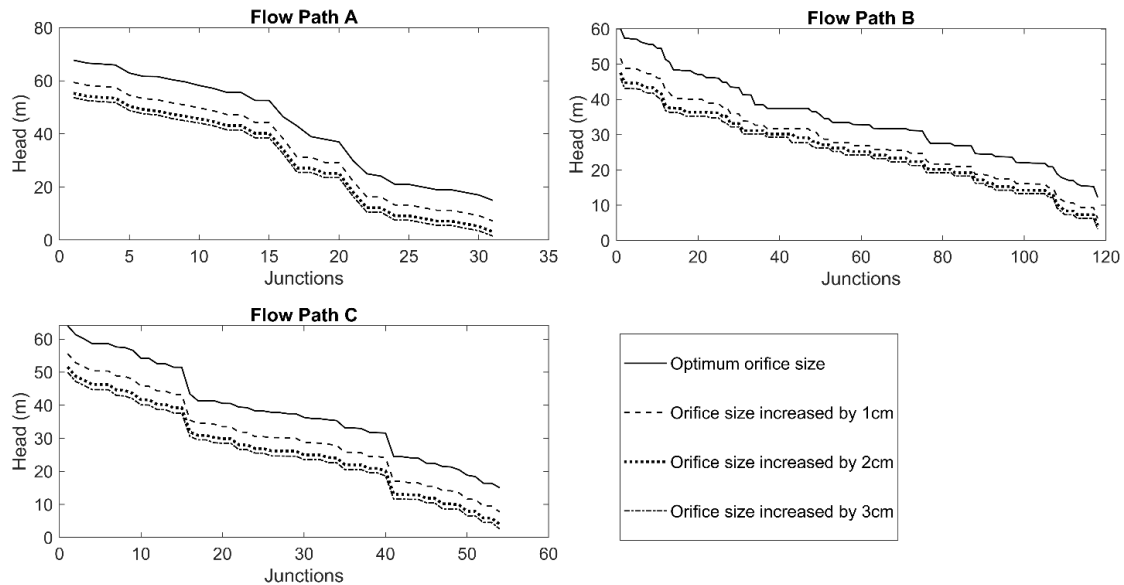
as shown in Fig. 14. Most of the nodes in flow path A and B consist of villas with low base demands while flow path

390

C consists of low to high rise buildings with high base demand. The resulting pressure variation established from these

391

flow paths for different orifice diameters under constant retention time are shown in Fig. 15.

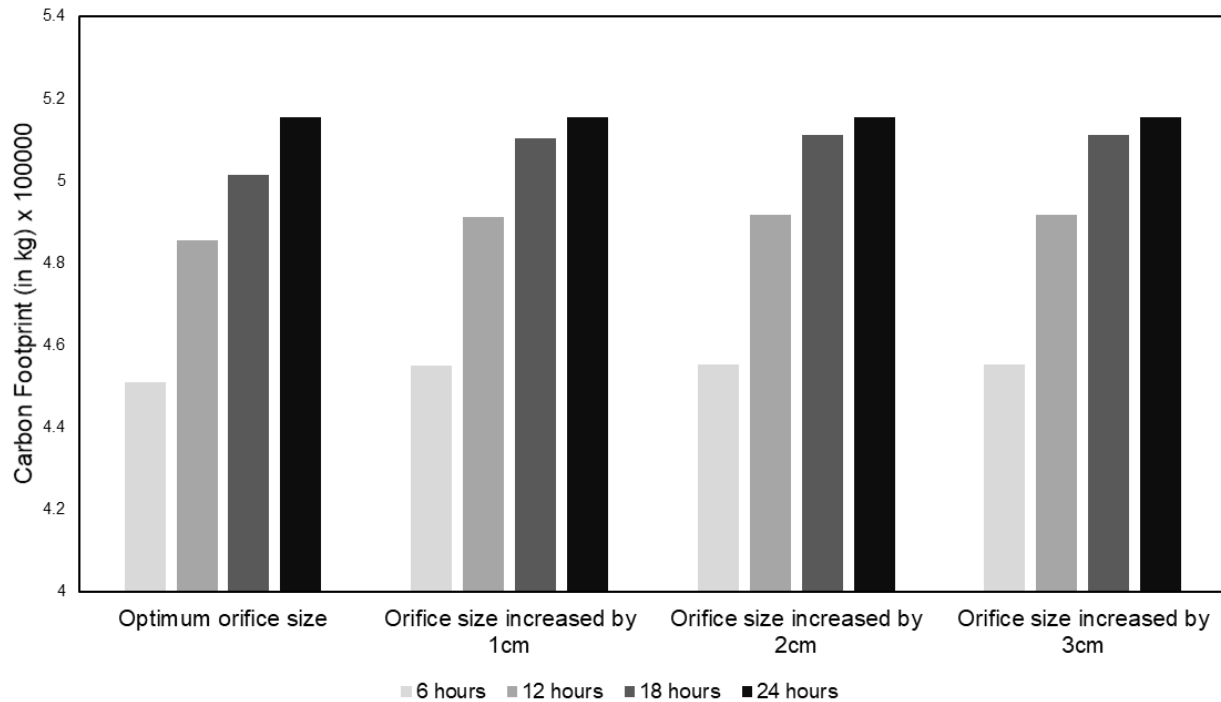


393 *Fig. 15 Head (pressure) changes on nodal junctions with increasing orifice diameters for each flow path*

394 For the given flow path in Fig. 15, the results indicated that the pressure drops with increasing orifice
 395 diameter. In fact, for flow path A, an increase in orifice diameter of 1cm results in a pressure drop close to 9m. Further
 396 increasing orifice diameter to 3cm for each nodal tank shows a change of approximately 15m. The drop in pressure is
 397 also higher for the junctions that had a larger optimum orifice diameter obtained from the reliability analysis (Table
 398 1). This is observed from flow path A and B where the difference in pressure decreases at the end of the flow path
 399 where the associated nodes type is villa. For flow path C, the nodal junction's types were relatively similar based on
 400 the demands, hence, the pressure drop with increasing orifice diameter remains constant along the path. Finally, it is
 401 worth noting the few discrepancies found in the flow path lines particularly when increasing the orifice diameter. It is
 402 observed that the curve in flow path A, B and C, do not follow a smooth pattern (pressure rises for some nodes
 403 downstream) when increasing the orifice diameters. This is because the orifice diameter for adjacent junction (that are
 404 not present in the flow path) increases. Hence, it changes direction of flow slightly and shows these few anomalies.

405 The final comparison is conducted by changing the retention time and orifice diameter of local tanks to
 406 observe the effect on the carbon footprint. The reliability analysis required both indicators to reach the value of '1' for
 407 the tanks to have an acceptable orifice and volume size. As such, when the orifice and volume size increases, the
 408 reliability values for both indicators would increase. This means the flow into the system would increase further which
 409 would increase the pump power consumption that would increase the carbon footprint. Any further increase in the

410 optimum orifice and volume size would not be reflected in the reliability indicator since the maximum value obtained
 411 is '1'. However, logically, if the size of the parameters is being increased, then it would only result in more pump flow
 412 that would utilize more carbon footprint.



414 *Fig. 16 Effect on carbon print with different orifice and volume sizes (retention time)*

415 In this analysis (Fig. 16), it was observed that increasing the orifice diameter with constant retention time (6
 416 hours) did not had a significant impact on carbon footprint. This is because the tank quickly reaches it full capacity
 417 within a few hours which causes the flow to become similar in all cases with different orifice diameter. On the contrary,
 418 increasing the retention time boosted the amount of carbon footprint produced as the tanks took relatively longer to
 419 fill up. Approximately, 10% of the carbon footprint has increased when the retention time is changed from 6 hours to
 420 24 hours. The results confirm that the footprint is proportional to the energy used by the pumps (i.e., a function of the
 421 power supplied by the pumps). Indeed, it had been observed previously that the power consumption increases with
 422 retention time, the carbon footprint also increases further. The result was accepted, but it should be noted that the
 423 actual carbon footprint will also account for the lifestyle of the area, temperature and greenhouse emission rate. It
 424 further suggests that the retention time should be kept low to avoid the production of larger carbon footprint.

425 **Conclusion:**

426 The strategy to find the optimum volume and orifice diameter would allow the engineers to improve the
427 current design of private tanks. As most of the associated code of practice recommends a 24-hour retention time for
428 local tanks is essential, this study shows that in fact the orifice diameter is much more significant parameter to be
429 optimized. Moreover, associating relatively high volume is not feasible as tank volume with 6 hours retention time
430 are observed to have enough capacity to satisfy the demand.

431 The results have shown the importance of reliability indicators as they can assess the performance of the
432 private tank by combining different factors that are affecting it. It is also found that there is a significant difference
433 between the two indicators (time-based and volume-based). The difference in their value is due to the weightage
434 provided by them. Nonetheless, each of them needs to reach the required reliability of 1 to satisfy the demand. These
435 indicators were effective in this case since they were able to predict the correct parameters of tank that would not lead
436 to failure by insufficient supply to the consumer, where others are not able to. However, they were not able to give
437 weightage to the parameters of pressure and quality, which can be the essence of developing new indicators that can
438 take these factors into account.

439 Overall, the results implied by the reliability indicators showed that the orifice and volume size of the tank is
440 influenced by the base demand and available pressure. In all the networks, where the tanks were initially empty, the
441 reliability value increases with the orifice diameters while changing the retention time did not had much impact. It
442 further indicated that the selection of the orifice and volume size should always be based on the worst-case scenario
443 (tanks are empty at the start of the simulation). In terms of carbon footprint and pressure, the results indicated that the
444 optimum orifice and volume size is the lowest value that reaches the required reliability. Any further increase in the
445 value (orifice and volume) would only increase the production of carbon footprint and head loss in the system.
446 However, these results do not include the impact on the water quality which should be analyzed for future studies.

447 **Data Availability:**

- 448
- 449 • Some or all data, models, or code that support the findings of this study are available from the
450 corresponding author upon reasonable request. This includes data for the sample network 1 with
all its characteristics.

- 451 • Some or all data, models, or code generated or used during the study are proprietary or confidential
452 in nature and may only be provided with restrictions. This includes the data for sample network 2
453 which is a real-time network that includes sensitive and personal details of the consumer.

454 **Acknowledgements**

455 WNetXL system used to run the simulation of all WDN models was provided by IDEA-RT s.r.l.
456 (www.idea-rt.com).

457 **References:**

- 458 Ackley, J. R. L. et al. (2001) Head-driven analysis of water distribution systems. Proc. Computer and Control in
459 Water Industry, Water software systems: theory and applications. Ulanicki, B. (ed.). Research Studies Press, UK,
460 183–192.
- 461 Adeloje, A. J., Soundharajan, B. S. and Mohammed, S. (2017) ‘Harmonisation of Reliability Performance Indices
462 for Planning and Operational Evaluation of Water Supply Reservoirs’, Water Resources Management. Springer
463 Netherlands, 31(3), pp. 1013–1029. <https://doi.org/10.1007/s11269-016-1561-x>.
- 464 Berardi, L., Laucelli, D. and Giustolisi, O. (2014) ‘Accounting for local water storages in assessing WDN supply
465 capacity’, in Procedia Engineering. <https://doi.org/10.1016/j.proeng.2014.02.017>.
- 466 Bhawe, P. R. (1981) ‘Node flow analysis of water distribution systems’, Journal of Transportation Engineering.
- 467 Carpentier, P., Cohen, G. & Hamam, Y. 1987 Water Network Equilibrium, Variational Formulation and
468 Comparison of Numerical Algorithms. Proc. Computer Application in Water Supply, vol. 1. J. Wiley & Sons, New
469 York, USA.
- 470 Chandapillai, J. 1991 Realistic simulation of water distribution system. J. Transp. Eng., 117, 258–263.
- 471 Cobacho, R. et al. (2008) ‘Private water storage tanks; Evaluating their inefficiencies’, Water Practice and
472 Technology. <https://doi.org/10.2166/wpt.2008.025>.
- 473 Collins, M., Cooper, L., Helgason, R., Kennington, J. & LeBlanc, L. 1978 Solving the pipe network analysis
474 problem using optimization techniques. Manage. Sci., 24(7), 747–760.

475 Criminisi, A. et al. (2009) 'Evaluation of the apparent losses caused by water meter under-registration in intermittent
476 water supply', *Water Science and Technology*. <https://doi.org/10.2166/wst.2009.423>.

477 Cross, H. 1936 Analysis of flow in networks of conduits or conductors. Bulletin n. 286, University of Illinois
478 Engineering Experimental Station, Urbana Illinois, USA, II, 1–29.

479 De Marchis, M. et al. (2011) 'Analysis of the impact of intermittent distribution by modelling the network-filling
480 process', *Journal of Hydroinformatics*. <https://doi.org/10.2166/hydro.2010.026>.

481 De Marchis, M., Freni, G. and Milici, B. (2016) 'Experimental Evidence of the Discharge Law in Private Tanks
482 Connected to Water Distribution Networks', in *Procedia Engineering*. <https://doi.org/10.1016/j.proeng.2016.07.428>.

483 De Marchis, M., Freni, G. and Milici, B. (2018) 'Experimental analysis of pressure-discharge relationship in a
484 private water supply tank', *Journal of Hydroinformatics*. <https://doi.org/10.2166/hydro.2018.135>.

485 Epp, R. & Fowler, A.G. 1970 Efficient code for steady-state flows in networks." *J. Hydr. Div.*, 96, 3–56.

486 Gargano, R. and Pianese, D., 2000. Reliability as tool for hydraulic network planning. *Journal of Hydraulic
487 Engineering*, 126(5), pp.354-364.

488 Germanopoulos, G. (1985) 'A technical note on the inclusion of pressure dependent demand and leakage terms in
489 water supply network models', *Civil Engineering Systems*. <https://doi.org/10.1080/02630258508970401>.

490 Giustolisi, O. & Walski, T.M. 2012 A Demand Components in Water Distribution Network Analysis. *J. Water
491 Resour. Plan. Manage.*, 138(4), 356 -367.

492 Giustolisi, O., Berardi, L. and Laucelli, D. (2012) 'Generalizing WDN simulation models to variable tank levels',
493 *Journal of Hydroinformatics*. <https://doi.org/10.2166/hydro.2011.224>.

494 Giustolisi, O., Berardi, L. and Laucelli, D. (2014) 'Modeling Local Water Storages Delivering Customer Demands
495 in WDN Models Accounting for Inline Tanks', *Journal of Hydraulic Engineering*.
496 [https://doi.org/10.1061/\(ASCE\)HY.1943-7900.0000812](https://doi.org/10.1061/(ASCE)HY.1943-7900.0000812).

497 Giustolisi, O., Savic, D.A. & Kapelan, Z. 2008a Pressure-driven demand and leakage simulation for water
498 distribution networks. *J. Hydr. Eng.*, 134(5), 626–635.

499 Giustolisi, O., Kapelan, Z. & Savic, D.A. 2008b An algorithm for automatic detection of topological changes in
500 water distribution networks. *J. Hydr. Eng.*, 134(4), 435–446.

501 Gupta, R. and Bhave, P. R. (1996) ‘Comparison of Methods for Predicting Deficient-Network Performance’, *Journal*
502 *of Water Resources Planning and Management*, 122(3), pp. 214–217. [https://doi.org/10.1061/\(ASCE\)0733-](https://doi.org/10.1061/(ASCE)0733-9496(1996)122:3(214))
503 [9496\(1996\)122:3\(214\)](https://doi.org/10.1061/(ASCE)0733-9496(1996)122:3(214)).

504 Isaacs, L. T. & Mills, K. G. 1980 Linear theory method for pipe network analysis. *J. Hydr. Div.*, 106, 1191–1120.

505 woMartin, D. W. & Peters, G. 1963 The application of Newton's method to network analysis by digital computers.”
506 *J. Inst. of Water Engrs.* X, 115–129.

507 Liserra, T., Maglionico, M., Ciriello, V. and Di Federico, V., 2014. Evaluation of reliability indicators for WDNs
508 with demand-driven and pressure-driven models. *Water resources management*, 28(5), pp.1201-1217.

509 Martínez-Rodríguez, J.B., Montalvo, I., Izquierdo, J. and Pérez-García, R., 2011. Reliability and tolerance
510 comparison in water supply networks. *Water resources management*, 25(5), pp.1437-1448.

511 McMahon, T. A., Adeloje, A. J. and Zhou, S. L. (2006) ‘Understanding performance measures of reservoirs’,
512 *Journal of Hydrology*. <https://doi.org/10.1016/j.jhydrol.2005.09.030>.

513 Mohamed, Hassan Ibrahim et al. (2019) Effect of roof tanks filling on the hydraulic performance of water supply
514 pipes network Available at: <https://www.researchgate.net/publication/336613877> (Accessed: 3 April 2020).

515 Piller, O. & Van Zyl, J.E. 2007 A unified framework for pressure-driven network analysis. *Proc. Water Management*
516 *Challenges in Global Change: Proceedings of Computer and Control in Water Industry (CCWI2007)*. Ulaniki, B.,
517 Vairavamoorthy, K. & Butler, D. (eds), Taylor & Francis, London, UK, 25–30.

518 Piller, O. & Van Zyl, J. E. 2009 Pressure-driven analysis of network sections via high-lying nodes. In: Boxal, J. &
519 Maksimovic, C. (eds). *Proceedings of Computer and Control in Water Industry*. Taylor & Francis, London, UK,
520 257–262.

521 Reddy, L. S. and Elango, K. (1989) ‘Analysis of water distribution networks with head-dependent outlets’, *Civil*
522 *Engineering Systems*. <https://doi.org/10.1080/02630258908970550>.

523 Rossman, L.A. 2000 Epanet2 Users Manual. US Environmental Protection Agency, Cincinnati, OH

524 Shamir, U. & Howard, C.D.D. 1968 Water distribution network analysis. *J. Hydr. Div.* 94, 219–234.

525 Tanyimboh, T.T. & Templeman, A.B. 2004 A new nodal outflow function for water distribution networks.” Proc.
526 4th International Conference on Eng. Computation Technology (CD-ROM), Civil-Comp Press, Stirling, UK, paper
527 64.

528 Tanyimboh, T.T., Tabesh, M. & Burrows, R. 2001 Appraisal of source head methods for calculating reliability of
529 water distribution networks. *J. Water Res. Plan. Manage.* 127(4), 206–213.

530 Todini, E. & Rossman, L.A. 2013 A unified framework for deriving simultaneous equations algorithms for water
531 distribution networks. *J. Hydr. Eng.* 139(5), 511-526.

532 Todini, E. (2011) ‘Extending the global gradient algorithm to unsteady flow extended period simulations of water
533 distribution systems’, *Journal of Hydroinformatics*. <https://doi.org/10.2166/hydro.2010.164>.

534 Todini, E. & Pilati, S. 1988 A gradient method for the solution of looped pipe networks. *Computer Applications in*
535 *Water Supply*, vol. 1. John Wiley & Sons, New York, 1–20.

536 Tucciarelli, T., Criminisi, A. & Termini, D. 1999 Leak analysis in pipeline systems by means of optimal valve
537 regulation. *J. Hydr. Eng.*, 125(3), 277–285.

538 Walski, T., 2003. *Advanced Water Distribution Modeling And Management*. Waterbury, CT: Haestad Press.

539 Wagner, J.M., Shamir, U. & Marks, D.H. 1988 Water distribution reliability: simulation methods. *J. Water Res.*
540 *Plan. Manage.*, 114(3), 276–294.

541 Wood, D.J., & Rayes, A.G. 1981 Reliability of algorithms for pipe network analysis. *J. Hydr. Div.*, 107, 1145–1161.

542

543

544

545

546

547 **Table Captions:**

548 Table 1 Optimum setting of the orifice and volume size for each type of node

549 **Figure Captions:**

550 Fig. 1 Actual scenario with private tanks, modified after (Giustolisi et al., 2014)

551 Fig. 2 Layout of a common underground private tank

552 Fig. 3 Schematic of Network 1, data from (Walski et al., 2003)

553 Fig. 4 Schematic of Network 2

554 Fig. 5 Impacts of orifice sizing on Volume (V is the volume, Q is the flow and d is diameter)

555 Fig. 6 Flow chart for the performed analysis

556 Fig. 7 Simulated storage for different retention times (orifice diameter constant at 2cm)

557 Fig. 8 Simulated storage for different orifice diameter of the private tanks (Volume size equivalent at retention
558 time of 6 hours)

559 Fig. 9 Simulated flow for tanks 4 and 6 with retention time of a) 6 hours b) 12 hours c) 18 hours and d) 24 hours

560 Fig. 10 simulated flow for tank 6 with changing orifice diameters

561 Fig. 11 Reliability analysis for each tank in the network

562 Fig. 12 Pressure variation with different orifice diameters for tank 6 and from DDA (without the inclusion of tanks)

563 Fig. 13 Carbon footprint comparison with different orifice and volume size for all tanks

564 Fig. 14 Flow path A, B and C for the DSO network

565 Fig. 15 Head (pressure) changes on nodal junctions with increasing orifice diameters for each flow path

566 Fig. 16 Effect on carbon print with different orifice and volume sizes (retention time)

567

568